

1 **Separation of an upwelling current bounding the Juan
2 de Fuca Eddy, off Vancouver Island**

3 **Jody M. Klymak^{1,2}and Susan E. Allen^{3,4}and Others**

4 ¹School of Earth and Ocean Sciences, University of Victoria, BC, Canada

5 ²Department of Physics & Astronomy, University of Victoria, BC, Canada

6 ³Department of Earth, Ocean and Atmospheric Sciences, University of British Columbia, Vancouver, BC,

7 Canada

8 ⁴Institute of Applied Mathematics, University of British Columbia, Vancouver, BC, Canada

9 **Key Points:**

- 10 • The shelfbreak current along Vancouver Island separates downstream of a submarine
11 bank.
- 12 • Offshore water is drawn onto the shelf and forms a sharp semi-persistent front with
13 the Juan de Fuca eddy.
- 14 • The Juan de Fuca eddy shows evidence of long residence times, and little evidence of
15 deep-water origin.

16 **Abstract**

17 Comprehensive water column observations of temperature, salinity, and oxygen on the
 18 productive southern Vancouver Island shelf offer a unique characterization of a number of
 19 processes affecting exchange on the shelf. A semi-permanent cyclonic “eddy” occupies the
 20 region in the lee of a bank where the shelf widens abruptly. The observations indicate that
 21 the water in this wide part of the shelf has distinct water mass properties, and is clearly
 22 a mixture of offshore water and water in a coastal current. The water in the “eddy” is
 23 either rapidly mixed (high κ), or has a long residence time (large τ), such that $(\kappa\tau)^{1/2} \sim$
 24 $50 - 100$ m. The offshore edge of this “eddy” water was very abrupt, with distinct water
 25 properties showing little lateral mixing between offshore and “eddy” water, with the front no
 26 more than 1-km wide. Previous work had hypothesized the role of a spur canyon incising the
 27 shelf in feeding water to the “eddy”; little evidence of this was found during the observations,
 28 however, these were collected during a relaxation and reversal of upwelling winds, which may
 29 have slowed the flow of water into the eddy. Tidal observations in the spur canyon also show
 30 very strong hydraulic flows in the cross-canyon direction accompanied by very high localized
 31 mixing rates in 50-m hydraulic jumps possibly exceeding $\kappa \sim 1 \text{ m}^2\text{s}^{-1}$. Upstream of the
 32 observation there is evidence of an along-shelf current flowing equatorward. This water
 33 is readily identified by partially mixed water properties, accumulated while on the shelf.
 34 This water is clearly observed to all separate from the shelf to a depth of approximately
 35 150 m, and is replaced offshore of the “eddy” by distinct offshore water. This event can
 36 be seen in sea-surface temperatures in satellite images as tongue of water that is ejected
 37 offshore, probably with the relaxation of upwelling, with the flow heading directly offshore.
 38 The cause of this offshore separation event are not determined, but likely include instability
 39 between the shelfbreak current and the California Undercurrent, and possible are catalyzed
 40 by separation from the abrupt underwater bank at the polward end of the study region.

41 **Plain Language Summary**

42 The southern Vancouver Island continental shelf is very productive due to high nutrient
 43 input from the Strait of Juan de Fuca and Salish Sea estuarine system, and substantial cross-
 44 shelf transport due to the complicated topography. The estuarine water flows poleward,
 45 hugging the coast as the Vancouver Island Coastal Current, and in the summer shelf water
 46 flows equatorward. Trapped between these two currents is the Juan de Fuca eddy, a stagnant
 47 region of water that occupies the shelf where it abruptly widens just north of the Strait of
 48 Juan de Fuca.

49 Here we present intensive sampling of the Juan de Fuca eddy region. The observations
 50 show the eddy is low in oxygen, and we find has undergone substantial vertical and lateral
 51 mixing. This indicates that the waters have a surprisingly long residence time for a coastal
 52 feature, and that this region extends the depth of the water column. In contrast to previous
 53 literature we find that the water likely has low oxygen from being used for respiration rather
 54 than being pulled from deep in the California Undercurrent.

55 The sampling also shows a remarkable flow separation of the equatorward shelf current
 56 The current is shown to detach and is pushed offshore. Such events are readily seen in
 57 satellite imagery, but the results here indicate that the separation extends the depth of the
 58 water column on the shelf, and that this separation may be partially driven by the local
 59 bathymetry. The separation is a very strong cross-shelf exchange event, and likely transports
 60 substantial nutrient-rich coastal water offshore to drive productivity in the deeper ocean
 61 adjacent to the continental slope.

62 1 Introduction

63 Cross-shelf exchange is important to the health and productivity of continental shelf regions, where oxygenated water is exchanged with nutrient-rich, but oxygen-depleted nearshore
 64 water. Cross-shelf transport usually requires ageostrophic flow, since balanced flow will tend
 65 to follow topographic contours, often providing a barrier to lateral exchange (Brink, 2016).
 66 Mechanisms for cross-shelf exchange include internal waves and instabilities in shelf-break
 67 fronts. Most-dramatically, however, topography can drive cross-slope exchanges, often seen
 68 most clearly in surface imagery, but occasionally observed *in-situ* (Barth et al., 2000).

70 Here we present detailed observations from the southern Vancouver Island shelf, collected
 71 in summer 2013, and sampled with a rapid profiling vehicle equipped with a CTD
 72 and oxygen sensor, supplemented by traditional hydrographic surveys. The shelf has
 73 complicated bathymetry figure 1, with a somewhat typical shelf poleward of our study site, but
 74 then widening in the lee of La Perouse Bank, and then hitting the Juan de Fuca canyon,
 75 equatorward. Water from the strait of Juan de Fuca flows poleward as a buoyant current
 76 that hugs the coast (Thomson et al., 1989; Hickey et al., 1991), while shelf water flows
 77 equatorward in the summer under upwelling conditions, both forced by local winds and
 78 via tele-connections with the long, homogenous shelves equatorward off Washington and
 79 Oregon (Hickey et al., 1991; Thomson & Krassovski, 2015; Engida et al., 2016). Trapped
 80 between these two currents is a region of relatively homogenous water that has been termed
 81 the “Juan de Fuca” eddy (Freeland & Denman, 1982; Freeland & McIntosh, 1989; Foreman
 82 et al., 2008; MacFadyen & Hickey, 2010).

83 One of our findings below is that the water in the deep pool of the Juan de Fuca
 84 eddy is either quite old or undergone significant vertical mixing. The low oxygen found in
 85 the Juan de Fuca eddy has caused it to be inferred to be upwelled from as deep as 400 m
 86 (Freeland & Denman, 1982; Dewey & Crawford, 1988). This inference was based on the
 87 oxygen being conservative, and hence having to come from close to the oxygen minimum
 88 zone found further offshore (Mackas et al., 1987). This lead to hypotheses that perhaps the
 89 eddy was fed by waters being drawn up a spur canyon of the Juan de Fuca canyon (called the
 90 Spur Canyon) via ageostrophic transport from offshore to onshore due to the low pressure in
 91 the eddy center (Weaver & Hsieh, 1987). Below, we will argue that there is not substantial
 92 evidence of such transport, and that oxygen is likely low because of consumption due to
 93 respiration.

94 A second important finding is that the water flowing equatorward along the shelf from
 95 upstream all detaches from the shelf and is pushed offshore to be replaced by offshore water
 96 that floods the southern shelf. Such events are important as they tend to transport nutrient
 97 rich shelf water out into the open ocean, fueling offshore ecosystems. Similar offshore motion
 98 has been remarked in the region using satellite images (Ikeda & Emery, 1984; Thomson &
 99 Gower, 1998), and observed further to the south off Cape Blanco (Barth et al., 2000),
 100 and other coasts (Relvas & Barton, 2005, e.g.). Net cross-shore transport of nutrients
 101 and chlorophyll have been found in hydrographic surveys off Vancouver Island (Mackas
 102 & Yelland, 1999), and associated with mesoscale features both in geostrophic velocities,
 103 and in satellites. The mechanisms driving such separations are poorly understood, but
 104 hypotheses include coastal hydraulics (Dale & Barth, 2001) leading to along-shore trapping
 105 of coastal waves, wind stress curl variations (Castelao & Barth, 2007), induced relative
 106 vorticity due to stretching of parcels that inertially overshoot their initial isobaths due to
 107 a sudden change in downstream bathymetry, and the non-linear breaking of large-scale
 108 meanders due to baroclinic instability between the wind-driven current and the California
 109 Undercurrent (Ikeda et al., 1984; Batteen, 1997).

110 In this paper we present observations from 2013 (section 2), presenting the data in
 111 a number of ways to highlight the important processes, with a focus on the offshore side
 112 of the eddy region (section 3) where we consider the age of the eddy, the steadiness of the
 113 front separating the eddy and the offshore water, properties along the spur canyon that

114 was believed to feed the eddy, and finally describe the large offshore separation of the shelf-
 115 break current and its intrusion into the interior. We discuss the origin of the eddy and the
 116 implications of the separating jet (section 4).

117 2 Site and Methods

118 Observations from three summer cruises in 2013 are discussed here. Two were hydro-
 119 graphic surveys carried out on the *CCGS Tully*, one in June, and the other in late
 120 September. The third was a finescale survey made in the Vancouver Island shelf between 21
 121 and 30 August 2013, aboard the *R/V Falkor*. The study site was the southern portion of the
 122 Vancouver Island Shelf (figure 1a), a particularly complicated region due to the bathymetry
 123 and varied forcing.

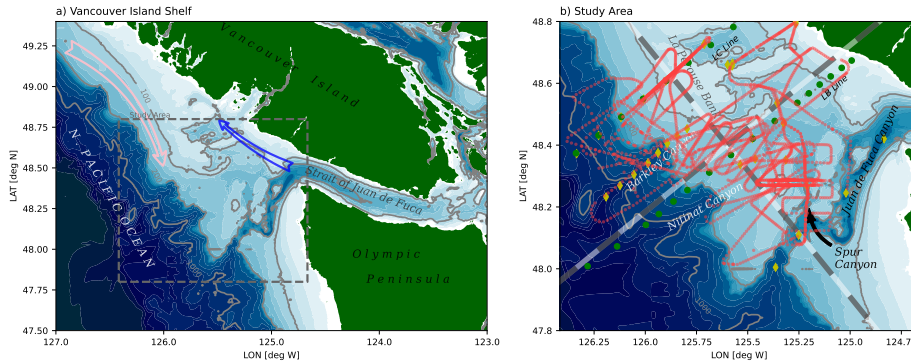


Figure 1. a) Study site on the Vancouver Island Shelf. The blue arrow indicates the direction of the Vancouver Island Coastal Current. The pink arrow indicates southward flow of the coastal upwelling current. The dashed box indicates the approximate limits of the study area. b) The study area with hydrographic casts from the La Perouse cruises along the LB and LC Lines are green dots, hydrographic casts during the Falkor cruise indicated in yellow dots, and Moving Vessel Profiler casts as red dots. The coordinate system used for this paper is shown with alternating grey and white bands at 10-km intervals.

124 At the south end of the study site is the Juan de Fuca canyon, which feeds dense water
 125 into Juan de Fuca Strait. This dense water is mixed with fresh water from the Fraser River
 126 at the sills and archipelagos further inland, and fluxes out the Strait again, where it turns
 127 poleward along Vancouver Island to form the Vancouver Island Coastal Current. The Juan
 128 de Fuca Canyon has a notable spur canyon (Spur Canyon), that incises the shelf towards
 129 the north into the study site (figure 1b). The rest of the shelf is punctuated by a series of
 130 banks and shallow basins. Notable is La Perouse bank, running along the shelf from the
 131 north, and moving isobaths offshore until it abruptly ends at around 48.5 N. The shelf break
 132 is characterized by a series of submarine canyons, in particular Nitnat Canyon and Barkley
 133 Canyon.

134 Observations from the LB and LC lines were collected aboard the *CCGS Tully* from
 135 2013-05-30 to 2013-05-31, which we will call “June”, and 2013-09-07 to 2013-09-09, which
 136 we will call “September”. These lines span the depths from about 50 m to deep offshore.
 137 The data comes from a lowered Seabird 9-11 CTD, with an SBE 43 oxygen sensor. Oxygen
 138 data have been checked against bottle casts, and the CTD corrected for sensor offsets and
 139 thermal lags.

140 Observations aboard the *R/V Falkor* were carried out from 2013-08-21 to 2013-08-30,
 141 starting two weeks before the September *Tully* cruise. Data were collected with an ODIM

142 Brooke-Ocean Moving Vessel Profiler, profiling to 200 m. The MVP was equipped with an
 143 AML Oceanographic CTD, and a Rinko Oxygen sensor with a 7-s response time foil. The
 144 MVP profiles at vertical fall speeds of 3 m s^{-1} to depths of 200 m or to within 5 m of the
 145 seafloor, whichever is shallower. Data collection took place while the ship cruised at speeds
 146 between 5 and 8 kts, usually at around 6 kts to enable fine horizontal spacing of the casts,
 147 with typical spacing less than 800 m. Data is collected during down- and up-casts, but is
 148 only reported for down-casts because the path through the water is highly asymmetric on
 149 the up-cast, whereas the downcast is largely vertical. The rapid speed of the profiling makes
 150 the oxygen measurements somewhat coarse, and probably biased due to the phase lag of
 151 the sensor, so we treat these largely qualitatively in this paper.

152 Unfortunately, neither vessel had an operational acoustic Doppler profiler during the
 153 cruises with which to make current measurements.

154 Winds during the cruises were typical for the west coast of Vancouver Island, with
 155 upwelling favorable winds during July and early August (figure 2). During the cruise, and
 156 for the week previous, the winds were intermittently downwelling favorable. Note that this
 157 locale is strongly affected by coastally trapped waves from further south, so doming of near-
 158 bottom isopycnals often persists despite local wind forcing (Thomson & Krassovski, 2015;
 159 Engida et al., 2016), and takes a finite amount of time to spin down.

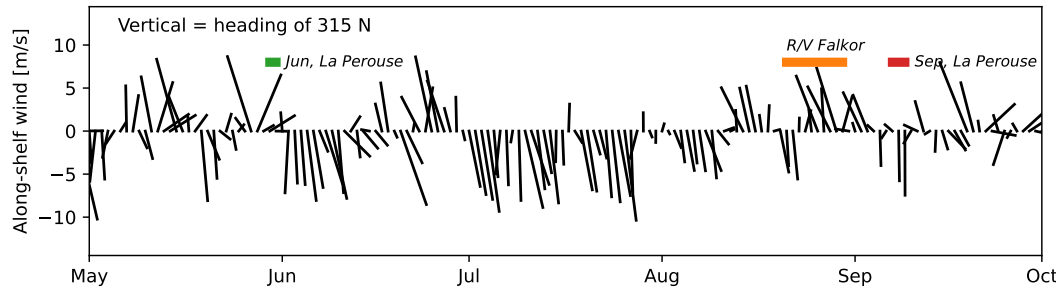


Figure 2. Wind from the La Perouse buoy (DFO, 2022). The vertical direction is along-shelf (chosen as a heading of 315 N). The wind components has been low-pass filtered to one-day averages. The timing of the cruises discussed in the paper are shown as colored bands.

160

3 Observations

161

3.1 Early and late summer broad-scale surveys

162

Hydrographic sections along the LB and LC lines highlight summer conditions on the
 163 Southern Vancouver Island Shelf, and indicate some of the features we are focusing on in this
 164 paper (figure 3). During both cruises and at both lines there is clear evidence of upwelling,
 165 with the 26.4 kg m^{-3} isopycnal reaching from 130 m to shallower than 85 m over the shelf.
 166 This dense water tends to be low in oxygen and cool. Further onshore, isopycnals tilt back
 167 down, and warm water fills the water column, evidence of the Vancouver Island Coastal
 168 Current that hugs the coast here.

169

The “Juan de Fuca Eddy” region is along the LB Line, mostly inshore of 0 km. This
 170 water is cooler and lower in oxygen than along the same isopycnal further offshore. Also
 171 note that during the June cruise the water in this region was cooler and more oxygenated
 172 than later in the summer during the September cruise. Near the surface, the isopycnals are
 173 domed, but the low-oxygen anomaly extends as high as the thin surface mixed layer.

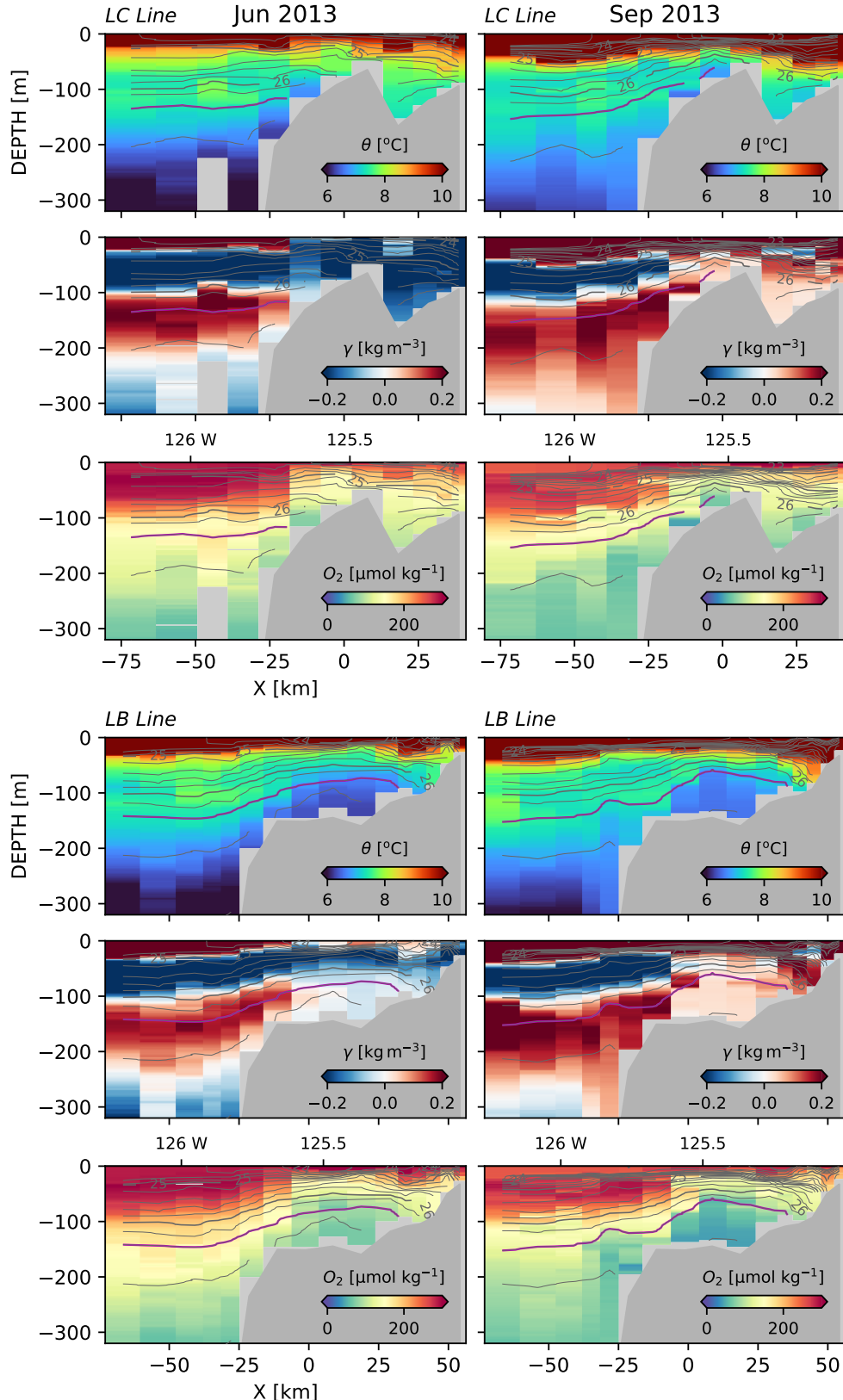


Figure 3. Observations along LC and LB lines in Jun and Sep 2013. X is across-shelf distance in the coordinate system shown in figure 1. Potential density is contoured every 0.2 kg m^{-3} , with the 26.4 kg m^{-3} . Potential temperature θ , salinity anomaly γ and oxygen concentration O_2 are colored for each section.

In contrast, the water upstream, along the LC line, does not show as much drawdown of oxygen, and is somewhat warmer, at least offshore of La Perouse bank (figure 3 top three rows). Water does not appear to make it over La Perouse bank into the basin onshore, or if it does, it does so intermittently. There appears to be some mixing of the deeper water and shallow water near 26.4 kg m^{-3} , with the water along this isopycnal becoming cooler and lower in oxygen where it intersects the shelf.

The θ - S properties show many of the features demonstrated above (figure 4a). Below 26.6 kg m^{-3} or so, the deep water masses are found offshore, and are largely homogenous. Shallower, there are distinct differences between the water found on the shelf and water found more offshore. These anomalies are hard to parse directly, so in this paper we use a spice anomaly, relative to a straight line in θ - S space (figure 4). The line passes the points $7.75^\circ\text{C}, 30 \text{ psu}$ and $6.6^\circ\text{C}, 35 \text{ psu}$, and spice anomaly for a given water sample at density σ_θ is $\gamma = \alpha(T - T_0(\sigma_\theta)) + \beta(S - S_0(\sigma_\theta))$ where $T_0(\sigma_\theta)$ and $S_0(\sigma_\theta)$ are the temperature and salinity along the mixing line at the same density as the water sample, with the sign convention that positive is warmer and saltier than data along the mixing line. It is hard to see from the θ - S plot in figure 4, but this mixing line is a strong feature of the water masses discussed in this paper.

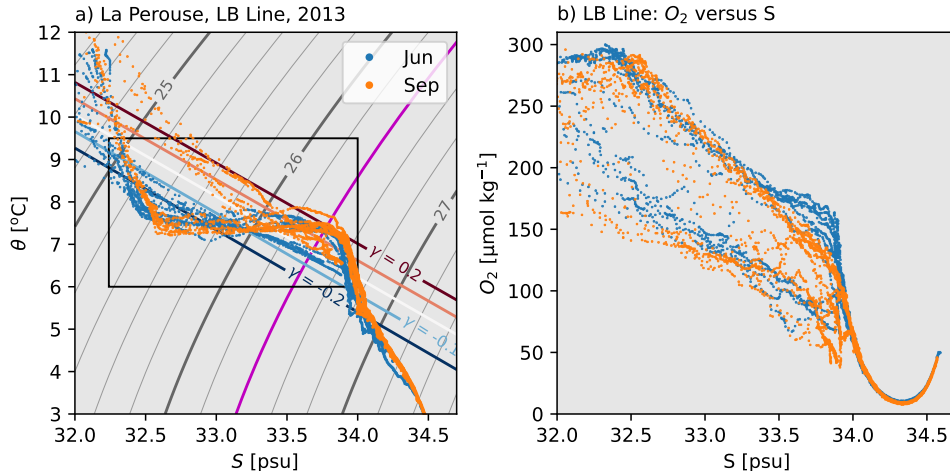


Figure 4. Potential temperature versus salinity for the La Perouse data shown in figure 3. Potential density is contoured in the same way. A definition of spice anomaly is shown in this plot, and discussed in the text. The rectangle is the θ - S range used in figure 5 below.

The spice anomaly defined this way is mapped in the middle row of each set of plots in figure 3. Offshore water tends to be high in absolute spice anomaly, with a positive-anomaly layer (red) centered at 26.4 kg m^{-3} sandwiched between negative-anomaly layers above and below. On the shelf ($-10 \text{ km} < X < 30 \text{ km}$), the distinct θ - S masses are attenuated and much closer to the mixing line than the offshore water. Hugging the coast ($X > 30 \text{ km}$), is the Vancouver Island Coastal Current, with a negative spice anomaly in June, and a positive anomaly in summer, consistent with the warming of this water during the summer.

The June and September cruises are quite similar in water properties, particularly in the offshore waters. Water has upwelled from deeper depths in September, but has most of the same water mass characteristics as earlier in the year. The water on the shelf is somewhat warmer than earlier in the year, and by September has started to fall off the mixing line.

203 In terms of oxygen, both cruises have a similar dichotomy between the onshelf and
 204 offshelf water, with water found in the eddy tracking at least $100 \mu\text{mol kg}^{-1}$ lower on the
 205 shelf than offshelf (figure 3, figure 4b). The very deepest water ($S \approx 33.9 \text{ psu}$) on the shelf
 206 shows a further $50 \mu\text{mol kg}^{-1}$ drop between June and September along the LB line.

207 3.2 Fine-scale surveys

208 3.2.1 Overview

209 As shown in figure 1, we conducted a large spatial survey of the shelf using the Moving
 210 Vessel Profiler, collecting over 2000 CTD casts in a relatively synoptic manner. This amount
 211 of data allows a reasonable census of the water masses that motivated our choice of the
 212 mixing line shown in figure 4. Binning in temperature and salinity, we can look at sample
 213 frequency of these observations figure 5, and we see that there are distinct water masses with
 214 few observations between them. Looking along the 26.4 kg m^{-3} isopycnal, we see that there
 215 is a large population along the mixing line. At the opposite extreme, we see that there is
 216 a large population with a positive spice anomaly of approximately 0.2 kg m^{-3} , representing
 217 the offshore water. Between these two end points there is a third water mass, somewhat
 218 indistinct from the offshore water mass, but very distinct from the water mass along the
 219 mixing line. These three water masses exist on deeper and shallower isopycnals as well,
 220 but become hard to distinguish from $\theta-S$ properties alone as the properties converge near
 221 26.1 kg m^{-3} .

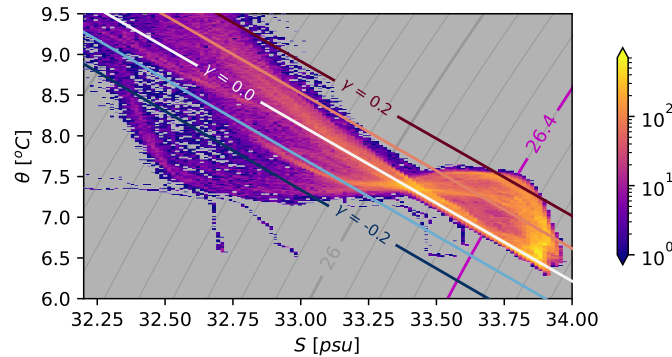


Figure 5. Sample density of salinity and potential density data from the cruise, with a logarithmic color scale. Grey contours are potential density relative to the surface, every 0.1 kg m^{-3} , and the magenta contour is the 26.4 kg m^{-3} isopycnal. Spice anomaly, γ is defined as temperature anomaly scaled by α along isopycnals from the mixing line found in the well-mixed region onshore, in kg m^{-3} .

222 These three water masses are quite coherent in space. While we did not do the specific
 223 La Perouse sections, our spatial coverage is such that we can make consistent synthetic
 224 sections (figure 6), taken at $y = 42, 28, 14$, and 0 km (see figure 1). During the August cruise,
 225 the upstream water along $\sigma_\theta = 26.4 \text{ kg m}^{-3}$ has moderate spice anomaly of $\gamma \approx 0.1 \text{ kg m}^{-3}$
 226 (figure 6a), and in this representation, the water appears "pink". There is some higher-
 227 anomaly water offshore of $x \approx -40 \text{ km}$ along this upstream section.

228 By $y \approx 14 \text{ km}$, this "pink" water along $\sigma_\theta = 26.4 \text{ kg m}^{-3}$ is gone and is replaced by
 229 high spice anomaly water $\gamma \approx 0.2 \text{ kg m}^{-3}$ ("red") that is directly next to well-mixed water
 230 ($\gamma \approx 0.0 \text{ kg m}^{-3}$, "white"), a situation that persists further down the shelf (figure 6c, d).

231 The onshore waters ($-5 < X < 40$ km) are remarkably well-mixed in θ - S space, despite
 232 still retaining significant density stratification.

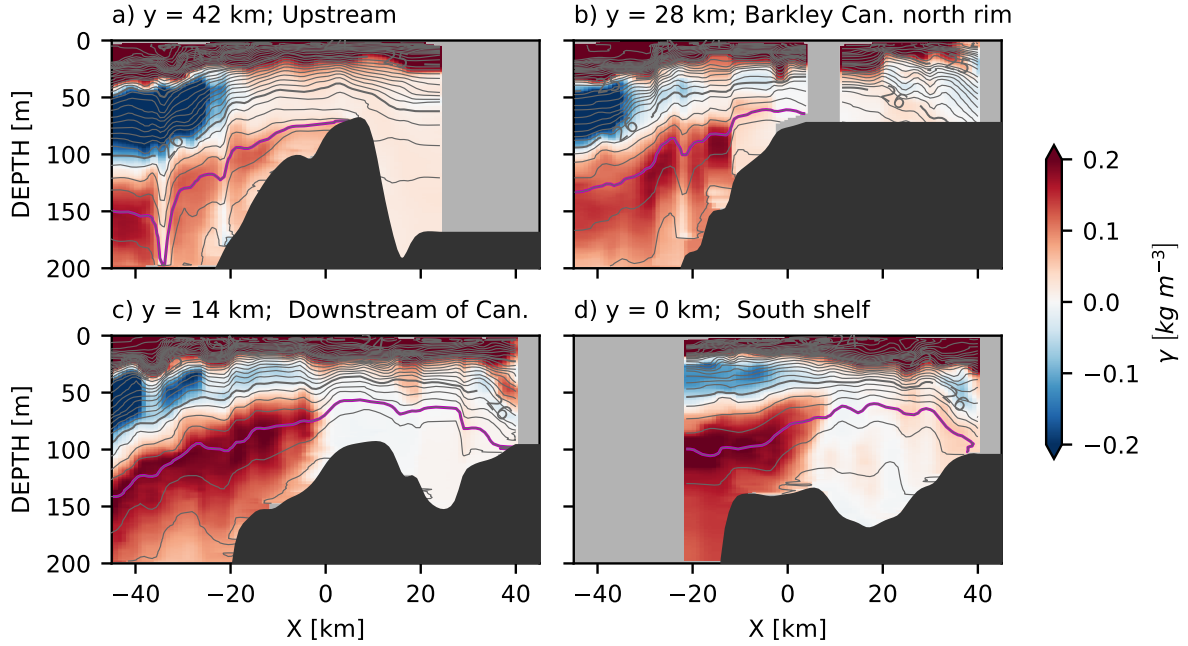


Figure 6. Synthetic sections of spice anomaly from the MVP data, projected along four lines from poleward (upstream of coastal current) a) to equatorward (downstream); the lines are shown in figure 1b). Isopycnals are contoured every $\sigma_\theta = 0.2 \text{ kg m}^{-3}$, with the $\sigma_\theta = 26.4 \text{ kg m}^{-3}$ isopycnal highlighted in magenta. Colors are spice anomaly as defined in figure 5. "BC" in panel (c) refers to Barkley Canyon.

233 Oxygen profiles, computed in the same manner, show similar trends, with the low-
 234 spice anomaly water clearly having a very low oxygen signature, while the strong negative
 235 spice anomaly shallower than $\sigma_\theta = 26.4 \text{ kg m}^{-3}$ has very high oxygen, and the deeper water
 236 is also more oxygenated. Of note is that compared with the coarser sampling along the
 237 LC Line (figure 3), we see that there is a very abrupt transition between the low spice
 238 anomaly/low-O₂ water and the offshore water over the "Eddy" region. We will see below
 239 that this transition is even sharper than indicated by these synthetic sections, since they
 240 alias some lateral and temporal irregularity in the θ - S -compensated front.

241 The spatial patterns are very clear when considering a map-view of properties along
 242 the $\sigma_\theta = 26.4 \text{ kg m}^{-3}$ isopycnal (figure 8). There is a region onshore of the south tip of La
 243 Perouse Bank (approximately 44.5 N, 125.75 W), that consists of water that is found along
 244 the mixing line (spice anomaly $\gamma \approx 0 \text{ kg m}^{-3}$) with low oxygen saturations; this water is called
 245 the Juan de Fuca eddy (or Tully eddy), though here an eddy shape is not readily apparent.
 246 Offshore of this region is water that is very warm and salty in comparison ($\gamma > 0.15 \text{ kg m}^{-3}$),
 247 and relatively high in oxygen (saturations of approximately 60%). The region between these
 248 two water masses is very abrupt, and is concave with respect to the isobaths on the shelf,
 249 stretching from La Perouse Bank to a shallow bank just above the Juan de Fuca canyon
 250 (48.3 N and 125.4 W).

251 Upstream of La Perouse bank, and Barkley Canyon, the water along the shelf has a
 252 weaker spice anomaly than the water further downstream ($\gamma \approx 0.7$, light pink colors). This

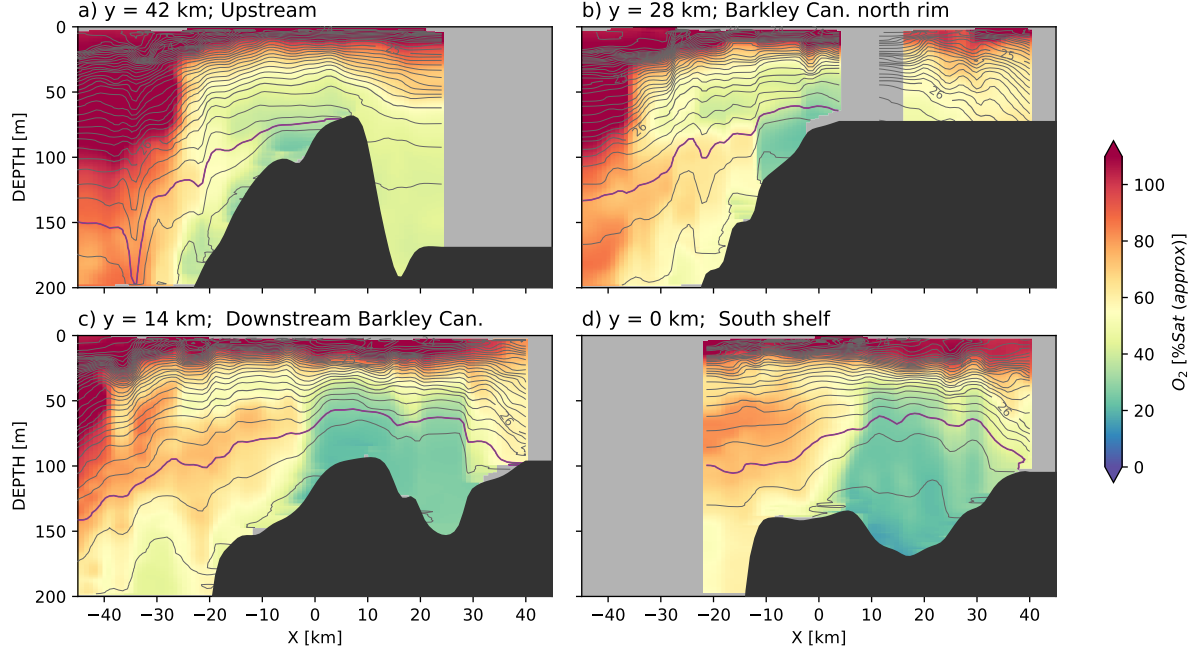


Figure 7. Synthetic sections of Oxygen, approximate percent saturation from the MVP data.

water is also somewhat lower in oxygen than water from offshore, though not as depleted as the water in the "eddy". This water appears to be pushed offshore just upstream of Barkley Canyon, and replaced on the shelf by the warmer offshore water.

3.2.2 Frontal survey

A systematic survey through the front between the offshore water and the "eddy" water demonstrates the structure of the front (figure 9). The survey started close to shore and passed through the Vancouver Island Coastal Current (casts 2030–2080). This water is buoyant and significantly fresher and cooler than water at the same density near the surface. There is strong evidence of isopycnal mixing of the surface water and the outflow water, with warm-salty water in the relatively wide front between the "eddy" water and the water in the current.

The front between the offshore water and the "eddy" water was passed through 10 times, showing its evolution following the along-shore equatorward flow. First, as noted in the composite sections, isopycnals slope up from offshore onto the shelf. This is in agreement with a shelf-break current, though the isopycnals flatten out in the "eddy" region. The front starts out very sharp, (along-track distance 50 km) though two small tendrils can be seen separating from the front on the inshore side. Similar tendrils are found on the second pass, perhaps a bit more separated from the front (≈ 80 km), and on the third pass (≈ 95 km). Note that these tendrils are made of up partially mixed water. The subsequent passes have more of this partially mixed water, such that the partially mixed region is up to 5-km wide by the fifth pass (≈ 150 km). However, note that deeper isopycnals retain a sharp front, and indeed the front appears sharp again by the seventh pass at all depths.

There is evidence of some warmer water swirling into "eddy", particularly along isopycnals deeper than 26.4 kg m^{-3} . Regions of warmer (and more oxygenated) water are found in tendrils at these depths (e.g. ≈ 170 km and ≈ 185 km).

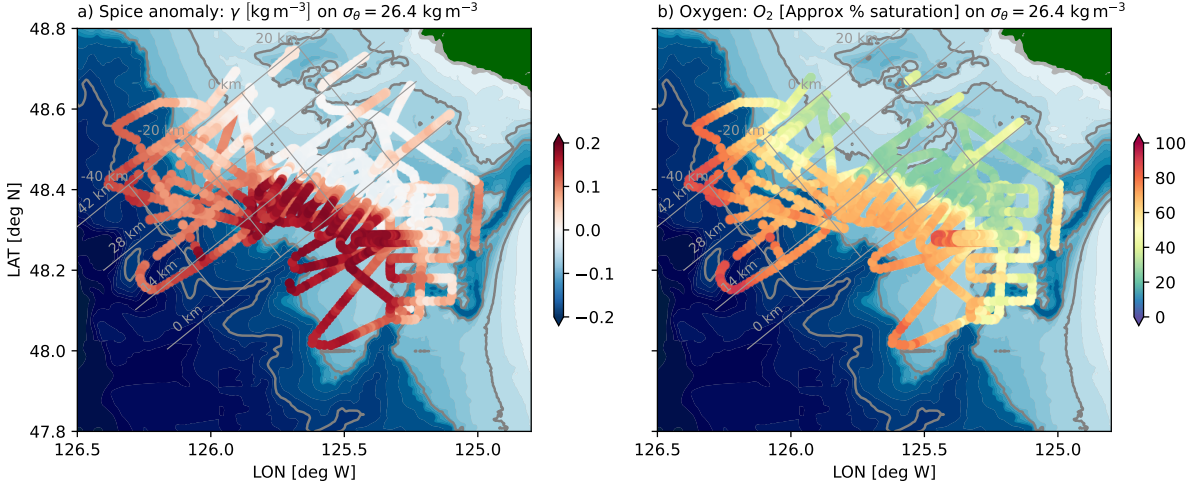


Figure 8. Spatial overview of a) local spice (temperature anomaly on an isopycnal: see text), and b) oxygen saturation on the $\sigma_\theta = 26.4$ kg m⁻³ isopycnal. Grey cross-slope lines are cross sections indicated in figure 6. Along-slope grey lines are every 20 km in the cross-slope direction, with $x = 0$ km near the 100-m isobath at the north end of the observation area.

The overall effect is similar to what was seen in the Gulf Stream with similar observations (Klymak et al., 2016); there are two quite distinct water masses, as seen in the θ - S plot (figure 9c). There is only a small population of samples between these two, indicative of substantial isopycnal and vertical mixing, but even these populations are relatively cut off from the large water masses, indicating that they are well-mixed on their own, in short episodic events.

3.3 Spur Canyon

The seasurface is low in the middle of the “Eddy”, so water has been hypothesized to move up the Spur Canyon due to ageostrophic motion (Weaver & Hsieh, 1987; Freeland & Denman, 1982). This is difficult to infer from water properties alone. Three transects up the canyon indicate that deep isopycnals slope up into the canyon (figure 10, to approximately 30 km). Across the eddy, isopycnals are largely flat until they intersect the Vancouver Island Coastal Current ($x \approx 80$ km). The deeper isopycnals do not make it into the deeper basin northeast of La Perouse bank ($x \approx 70$ km).

Water properties along the canyon go from modified offshore water, to eddy water, with a relatively consistent transition at about 30 km. Oxygen behaves in a similar manner, though some of the incoming water has slightly lower oxygen than water inside the eddy (not shown). Based on these sections, it is difficult to infer water motion up the canyon in particular.

Much of the modified water in the Spur Canyon appears to come from the shelf to the west, but heavily modified by tidal mixing. A repeated tidal survey over the bank on the west side of the canyon shows a strong hydraulic response (figure 11) during onshore flow (17:58–21:00). Note the tide here is largely diurnal, so this onslope flow only occurs once a day. Given the stratification of $N \approx 6 \times 10^{-3}$ rad s⁻¹ and an overturning scale of 50 m, we might expect dissipation rates reaching $\epsilon \sim L^2 N^3 \approx 5 \times 10^{-4}$ m² s⁻³, which is more than three orders of magnitude higher than dissipation observed west of this location by (Dewey & Crawford, 1988). In terms of a diapycnal diffusivity $\kappa = \gamma\epsilon/N^2 \approx 1$ m² s⁻¹, assuming a

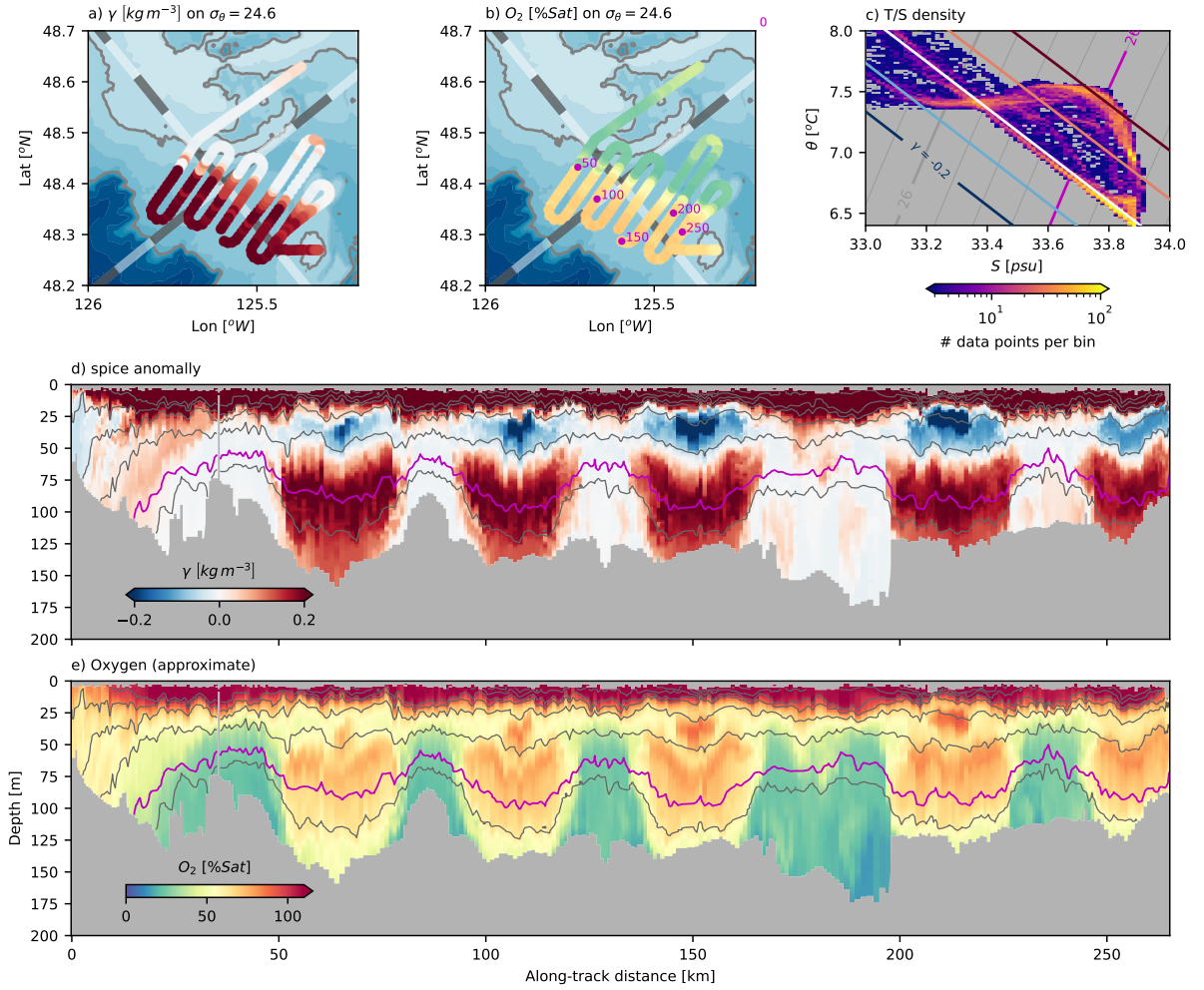


Figure 9. Data from a survey focusing on the front region (2013-08-28T15:11 to 2013-08-29T09:18) a) spice anomaly along 26.4 kg m^{-3} . Grey-white alternating lines are the coordinate system, with 10-km alternating shades. b) oxygen saturation; magenta dots correspond to distance along-track. c) density of data points (logscale) in this section of data. d) cross-section of spice anomaly along track. Grey isopycnals are contoured every 0.5 kg m^{-3} , and the 26.4 kg m^{-3} isopycnal is shown in magenta. e) cross-section of oxygen saturation.

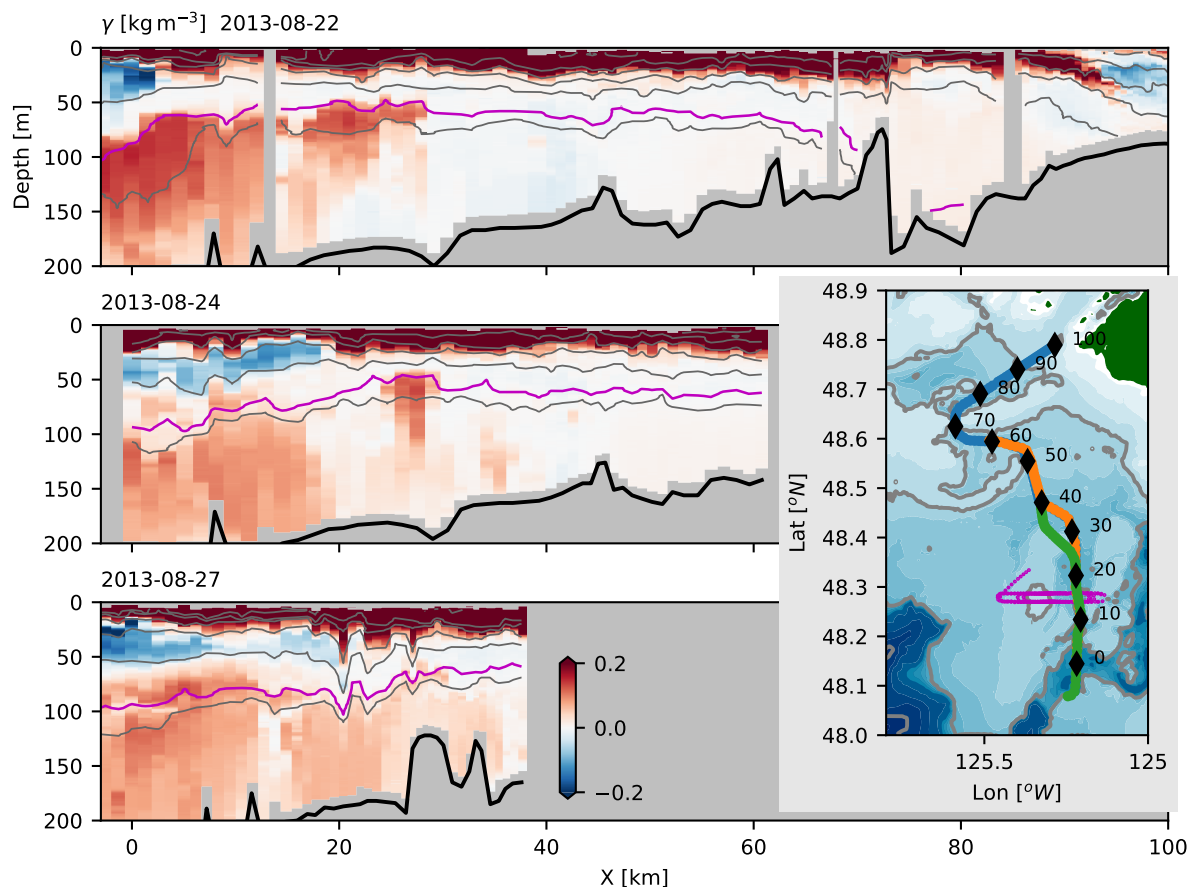


Figure 10. Magenta line in map inset is path taken during a cross-canyon survey.

305 mixing efficiency of $\gamma = 0.2$. The effect on the properties in the canyon is for water to spill
 306 over from the offshore front into the canyon during the tide. This water is rapidly mixed
 307 with surrounding water such that its strong offshore spice values are attenuated.

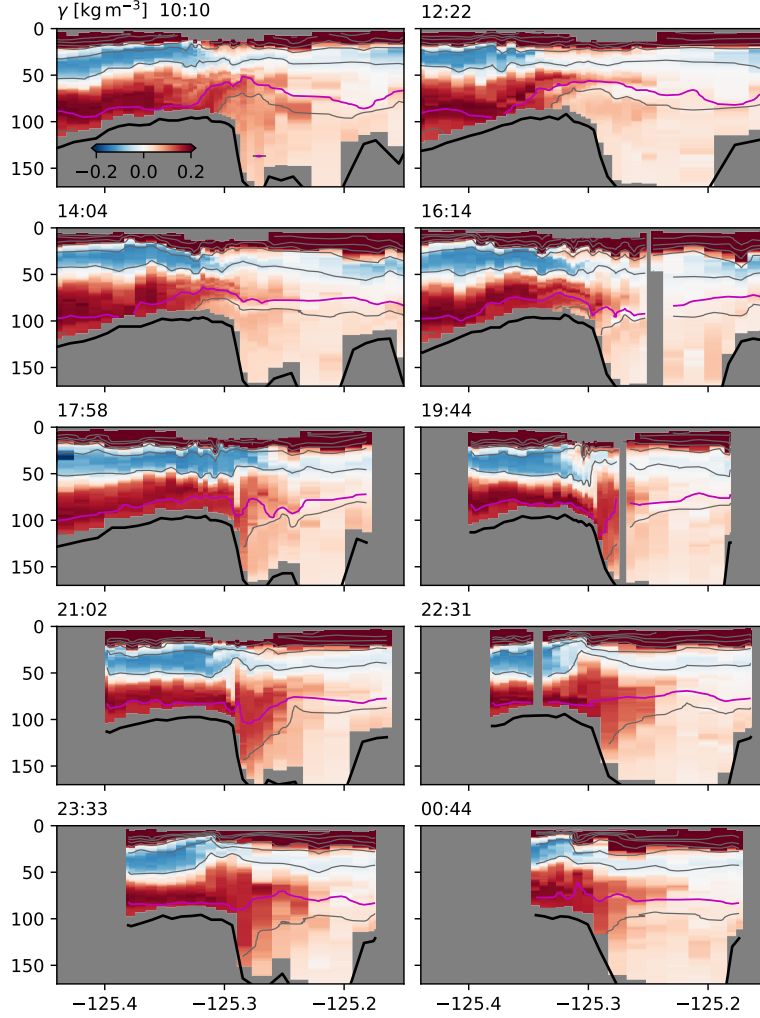


Figure 11. Repeated, tide-resolving survey across the Spur Canyon, time is indicated in the upper left of each plot (29 August, 2013).

308 This cross-canyon mixing makes it ambiguous if there is water moving up the canyon
 309 or not. There is indeed a general tendency along the canyon for higher spice water to be
 310 found offshore (figure 10) but it seems likely the source of the higher spice is over the bank
 311 rather than water being advected up the canyon.

312 3.4 Offshore tongue

313 The very narrow front on the offshore side of the “eddy” region persists, despite there
 314 being considerable “intermediate” water found upstream along the shelf. This water must go
 315 somewhere (or be accelerated unreasonably fast in the frontal region), and indeed it appears
 316 to largely be pushed offshore just upstream of Barkley Canyon (figure 12). There is a tongue
 317 of partially mixed (γ is pink along 26.4 kg m^{-3}) that flows almost due south just west of 126
 318 W. We had trouble crossing the whole tongue with the scale of our surveys, but it is at least

319 30 km wide. It also appears to end at approximately 48.2 N. This partially mixed water
 320 reaches from relatively shallow isopycnals to at least 26.6 kg m^{-3} (figure 12, left panel).
 321 Unfortunately, we cannot track the fate of the isopycnals deeper than this because they tilt
 322 down offshore, below the depth limit of the MVP. The shallower isopycnal appears to have
 323 the tongue closer to the shelf than at 26.4 kg m^{-3} , indicating strong three-dimensionality to
 324 this feature.

325 This feature is embedded in the larger scale isopycnal tilt caused by the upwelling
 326 (figure 12 right panels), so it is difficult to see dynamically what is driving this offshore
 327 push. One possibility is that it is simple flow separation as the water is not able to make the
 328 sharp turn around Swiftsure Bank. Whatever causes it, the water downstream is replaced
 329 by offshore water with much higher sigma values.

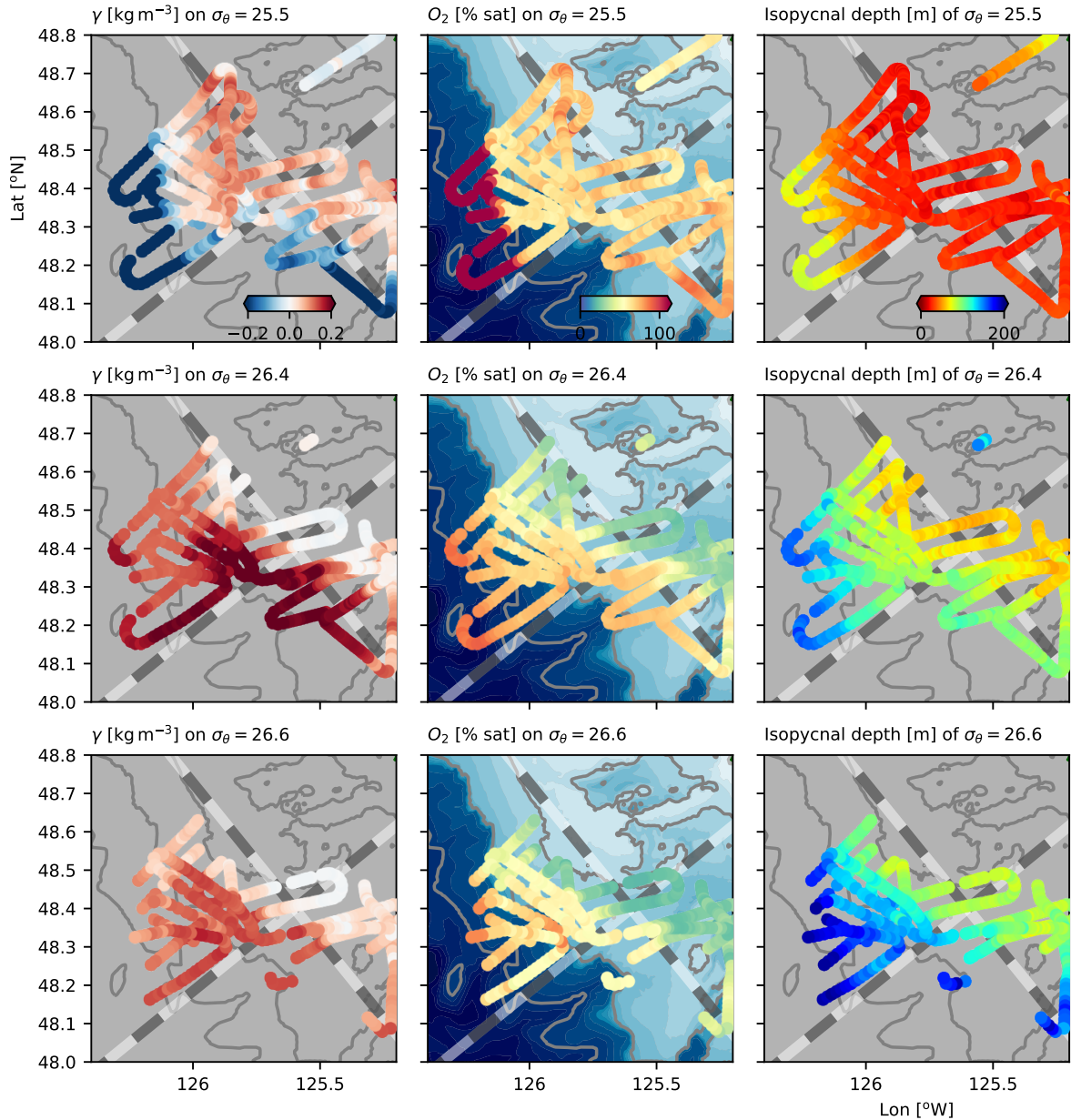


Figure 12.

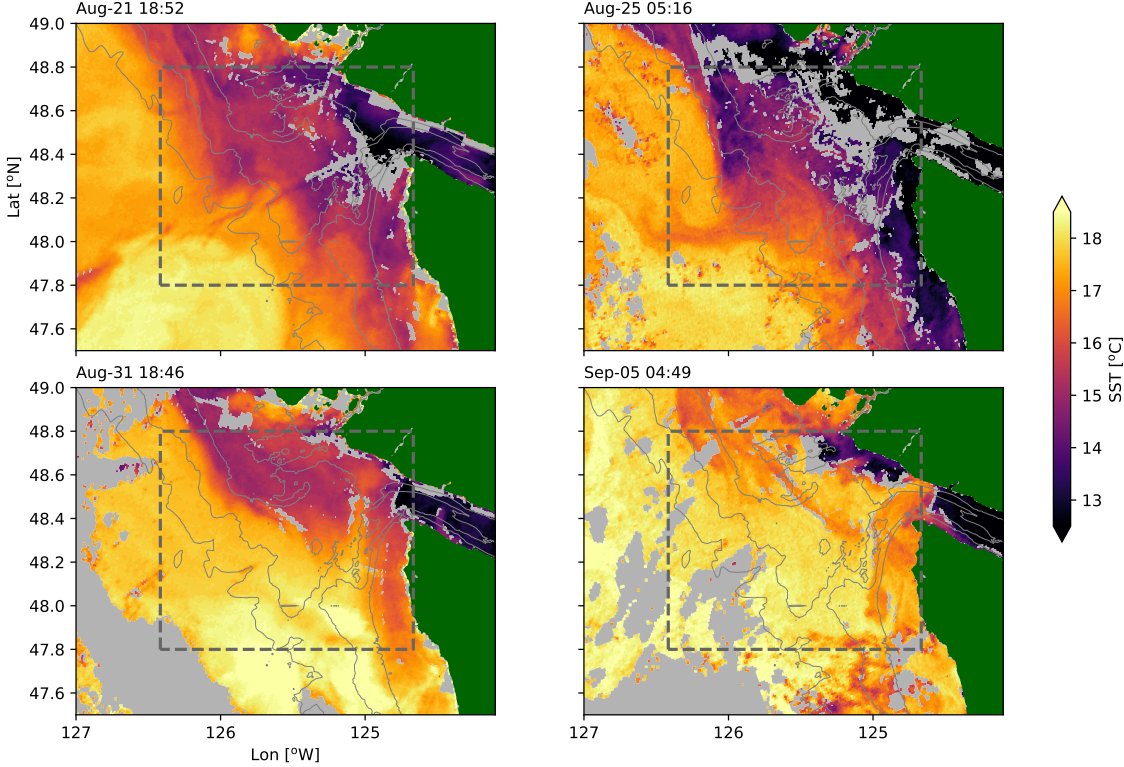


Figure 13. Sea surface temperature images from the observation period. Grey areas are clouds; dashed gray line is the study area. Depths are contoured in thin gray lines at 200, 150 and 100 m. (OSI SAF, 2015)

We can attempt to track this feature in satellite imagery, though there are lots of clouds during this time period. Sea-surface temperatures are generally colder coming out of the Strait of Juan de Fuca (figure 13). Water flowing equatorward along the shelf tends to be cooler than offshore water, though this water is significantly saltier than the Juan de Fuca water hugging the shelf. On Aug-25, there is a cold tongue of water separating from La Perouse bank, and pointing south at 125.8 W with a cooler tendril streaming west at 48 N. This feature is not as well-developed in the previous image, Aug 21, perhaps indicating that it is an evolving mesoscale feature. By 31 Aug, there is no surface expression of the feature, though tendrils of cooler water can be seen separating from La Perouse Bank. By Sep-05 the water gas significantly warmed, but the offshore pushing anomaly does not appear to have a surface signature.

Ccean chlorophyll estimates show the same feature (figure 14) demostrating the advection of a region of high chlorophyll to the west side of the eddy. It also shows a relatively high-chlorophyll squirt to the west, again exiting the study region at approximately 48 degrees N. The feature is relatively long-lived, on the order of one month. Inspection of images before 2013-08-05 were too obscured by clouds, or did not show this feature, and even by 2013-09-06 we see the feature fading from the satellite. However, note that this feature is somewhat south of tongue that we observe deeper in the water column, but is indicative of substantial offshore transport in the region.

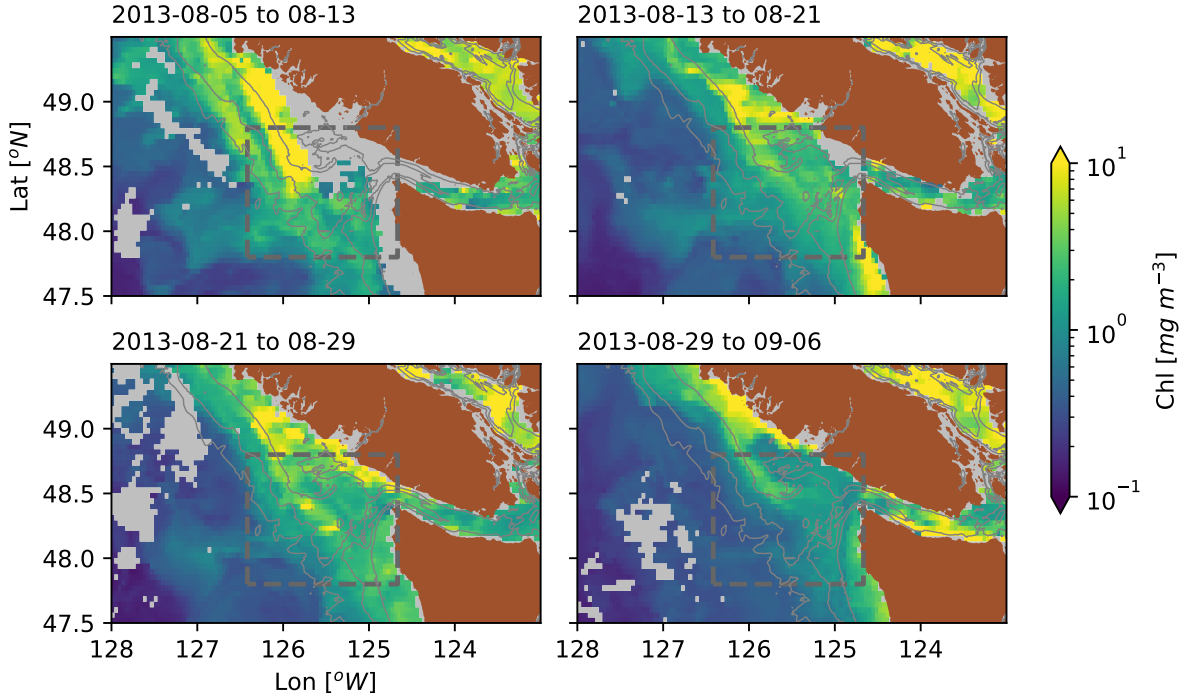


Figure 14. Surface chlorophyll density estimated from ocean color (Hu et al., 2012; NASA Ocean Biology Processing Group, 2017) over 8-day windows in 4-km bins. Gray regions had too many clouds for acceptable averages.

4 Summary and Discussion

The results of this fine-scaled survey perhaps pose more questions than they answer, but the questions are important to set the processes that should be looked for in understanding the circulation of the southern Vancouver Island shelf.

4.1 Age and source of the eddy water

The water we have been referring to as the Juan de Fuca Eddy is a relatively well-mixed water mass, as evidenced by the water therein lying along a mixing-line in θ - S space relative to water offshore (figure 4 and figure 5). Water coming equatorward along the shelf is closer to offshore water, though also shows clear signs of modification due to mixing.

Unfortunately, this data set cannot definitively track where the water in the eddy originated from. The deepest water in the eddy could originate along the θ - S line from approximately 5.5 degrees to 7.5 degrees (figure 4a), which in the open ocean spans depths from 420 m to 70 m. Mackas et al. (1987) attempted to determine the origin of the water by including oxygen as a third variable to resolve the ambiguous θ - S relation. However, as figure 4b makes clear, oxygen is definitely not a conserved property in the eddy, with concentrations up to $150 \mu\text{mol kg}^{-1}$ lower in the eddy than the water found offshore, and in a way that definitely cannot result from conservative mixing. As a best guess, if the water in the deepest part of the eddy came from a vertical mixture of the water at 26.5 kg m^{-3} and an equal distance down in density space of 26.7 kg m^{-3} , then the deepest water in the eddy would be coming from a depth of 250 m. This is actually a relatively typical upwelling depth for coastal flows, and may not require extra input up Spur canyon as posited by Freeland and Denman (1982).

We found little evidence of vigorous flow up the Spur Canyon, or if there is, then the mixing in the canyon is quick enough to remove the θ - S signature of offshore water within 20 km (figure 10). We did find substantial evidence of mixing in the canyon, but the primary route of high-salinity water into the canyon appears to be due to tidal flow over the banks on the west side (figure 11), rather than evidence of flow up the canyon. However, it is also of note that upwelling winds had ceased at this point (figure 2), meaning that the offshore pressure gradient may be reduced, leading to less ageostrophic upwelling in the canyon. Whether the cessation of winds would also lead to a reduction of the low sea level height in the center of the eddy is an open question.

There is evidence of aging of the water in the eddy between late spring and late summer (figure 3), with a reduction of oxygen in the eddy. If we posited that the reduction was all from the same water, then the oxygen consumption rate over the time between the late-May and early September cruises would be on the order of $0.5 \mu\text{mol kg}^{-1}\text{d}^{-1}$. This seems on the low side of continental upwelling system estimates of apparent oxygen utilization rates, which are between 1 and $5 \mu\text{mol kg}^{-1}\text{d}^{-1}$ (Dortch et al., 1994). So it seems possible the eddy has enough exchange with the surrounding water to have a shorter residence time.

There is partial mixing of the water in the eddy, though it remains vertically stratified, and the amount of homogenization is such that either the mixing is very strong, or the water is retained in the eddy for a long time. The amount of turbulence required to homogenize 100 m of water over 90 days is $\kappa \approx 10^{-3} \text{ m}^2 \text{s}^{-1}$. Given that the diffusivity implied in the cross-channel surveys was (very) locally on the order of $\kappa_\rho = 10 \text{ m}^2 \text{s}^{-1}$, this number is not outrageous if we think that such high dissipation is found in 10^{-4} of the water column. We can more carefully quantify this by considering a synthetic profile of temperature and salinity based on an offshore profile, extrapolated from the bottom of the 200-m cast to 250 m, assuming that the temperature and salinity at 250 m are $6.2 [\text{°C}]$ and 34 psu respectively (figure 15). Water at the offshore station was warmer than onshore, so the profile was also linearly interpolated to a surface value of (31.6 psu, 12 °C). The profile was then linearly compressed into a depth of 150 m representative of the shelf depth in the dense pool, and subjected to mixing with a constant diffusivity of $\kappa = 10^{-3} \text{ m}^2 \text{s}^{-1}$, with the surface and bottom values pinned under the assumption that the near-bottom source and surface waters are replenished from a large reservoir. Similar to the naive scaling, the T-S relationship does not approach a straight line until after approximately 60-100 days, or until the mixing affects a vertical length scale of $\lambda = (\tau\kappa)^{1/2}$ that is greater than $\approx 70 \text{ m}$.

The sharpness of the front with the eddy and the offshore water is also intriguing. It was persistent for the duration of our detailed survey (figure 8), and, so far as we can tell with the limited resolution, was present during the La Perouse cruises. There is not any substantial bathymetry blocking the onshore incursion of water at this location, so there must be a dynamic barrier. In contrast, numerical simulations of this region reported by (Sahu et al., 2022) using a NEMO 36th-degree regional model indicate that there is relatively rapid exchange between the deep eddy water and the rest of the coastal ocean. In this model, the region where the eddy resides has velocities equal or greater than other parts of the shelf, and water has an approximate residence time of less than 20 days. Consequently, the eddy water does not develop a distinct θ - S signature from the surrounding water.

Overall, it would be an improvement to our understanding of the eddy if we could sample the shelf more persistently. The eddy was already well-formed by the June La Perouse cruise, and seems to evolve slowly during that time. Capturing its formation, presumably earlier in the spring, and its evolution through the year would be valuable in understanding retention and exchange on this productive part of the shelf.

4.2 Offshore exchange of shelf water

The (apparent) displacement of shelf water from La Perouse Bank is relatively dramatic. Eddies have been known to separate from irregular coastal topography, both at the

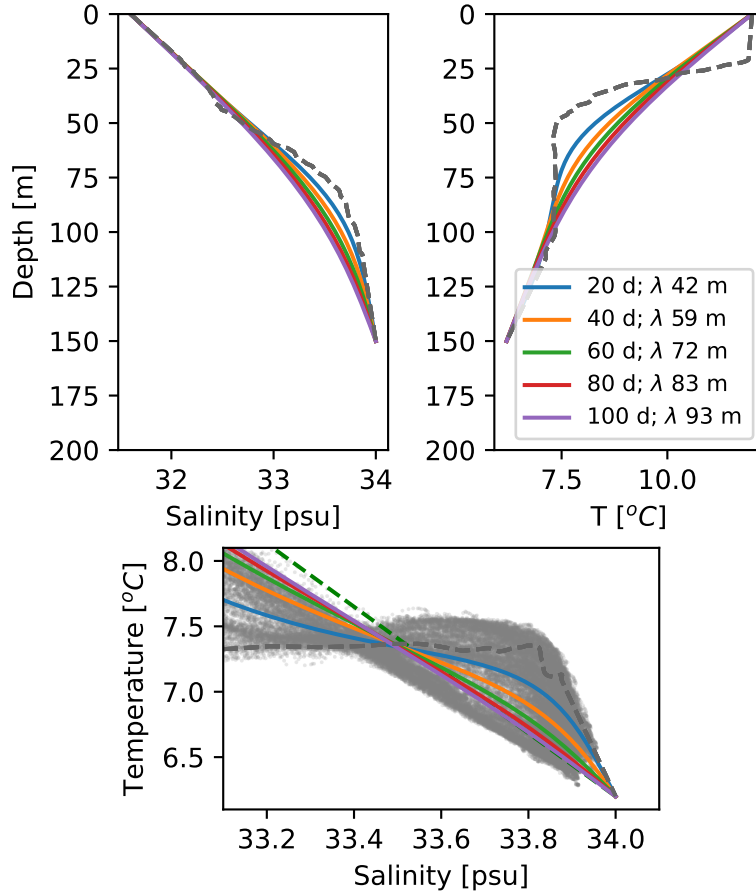


Figure 15. Mixing model assuming constant eddy diffusivity of $\kappa = 10^{-3} \text{ m}^2 \text{s}^{-1}$ acting on an offshore temperature and salinity profiles compressed from 250 thick to 150 m thick. Profiles are pinned to the deep value at (34 psu, 6.2 $^{\circ}$ C), and a shallow one at (31.6 psu, 12 $^{\circ}$ C).

surface (Barth et al., 2000), and deeper in the water column (Pelland et al., 2013). It has been recognized that instabilities lead to exchange between the open ocean and the shelf at this location (Ikeda & Emery, 1984, 1984). However, observations of the wholesale replacement of shelf water by a new water mass from offshore, is relatively rare. In our situation it is clear that water from as deep as 150 m is separating from the shelf and moving offshore (figure 8, figure 12).

Satellite imagery makes it clear that there is often an exchange between coastal and deepwater along the Vancouver Island shelf (figure 16). Most years there are three or four large excursions from the shelf into the open ocean, many of them over 100 km long. The lengthscale in these images is somewhat larger than that inferred for this region by Ikeda et al. (1984). It is possible that there is even some spatial locking of these features, with a persistent separation at the north tip of the Island, and a strong tendency for one at 49.5 N. Our study area also has evidence of a squirt in most of the years, with 2011 being the only clear exception. General baroclinic instability of the upwelling front is a possible mechanism to drive offshore exchange (e.g. Ikeda et al., 1984; Durski & Allen, 2005), but this tends to be shallow, with smaller-scale instabilities that will not extend as far into the interior ocean as observed here. Rather it seems likely that the topographic change engendered by the sudden turn to the east of La Perouse bank catalyses a larger scale instability at this location. In Durski and Allen (2005), when including realistic shelf bathymetry including Heceta Bank, the region around the bank catalyzes intermittent large-scale instabilities similar to the feature here and along the coast (Battieen, 1997).

Large-scale mixing between the shelf and open ocean has been evident since the satellite era. Here we demonstrate that the flow is originating on the shelf and separating from the bathymetry and being injected into the interior down to the bottom of the water column. A similar observation was made by Barth et al. (2000) downstream of Cape Blanco, Oregon, where the coastal current was observed to detach from the shelf in the lee of the cape, and squirt into the interior. They hypothesized that as the current moved offshore, it deepened, stretching isopycnals and creating cyclonic relative vorticity that would tend to push the current back onshelf, but then it was caught in the undercurrent and stalled, being pushed offshore. It is also possible that coastally trapped waves in the region experience a hydraulic control, and these meanders are the response (Dale & Barth, 2001).

Regardless of the dynamics, the offshore transport is substantial. If we assume the coastal current is approximately 0.1 m s^{-1} over 100 m in the vertical and 20 km in the horizontal, it represents 0.2 Sv of nutrient- and chlorophyll-rich shelf water transported offshore. Our observations are a finer detailed representation of the kind of cross-shore transports inferred by Mackas and Yelland (1999) from hydrographic surveys, and definitively show that this water can originate from the shelf from relatively deep depths and be transported offshore. We do not have velocity measurements for the water that replaces it, but assuming that water also flows along-shelf, there is a large replacement of low-O₂, low-nutrient water with offshore water at this location. This emphasizes the importance of three dimensional observations and modeling of cross-shelf dynamics when thinking about biological processes on the shelf.

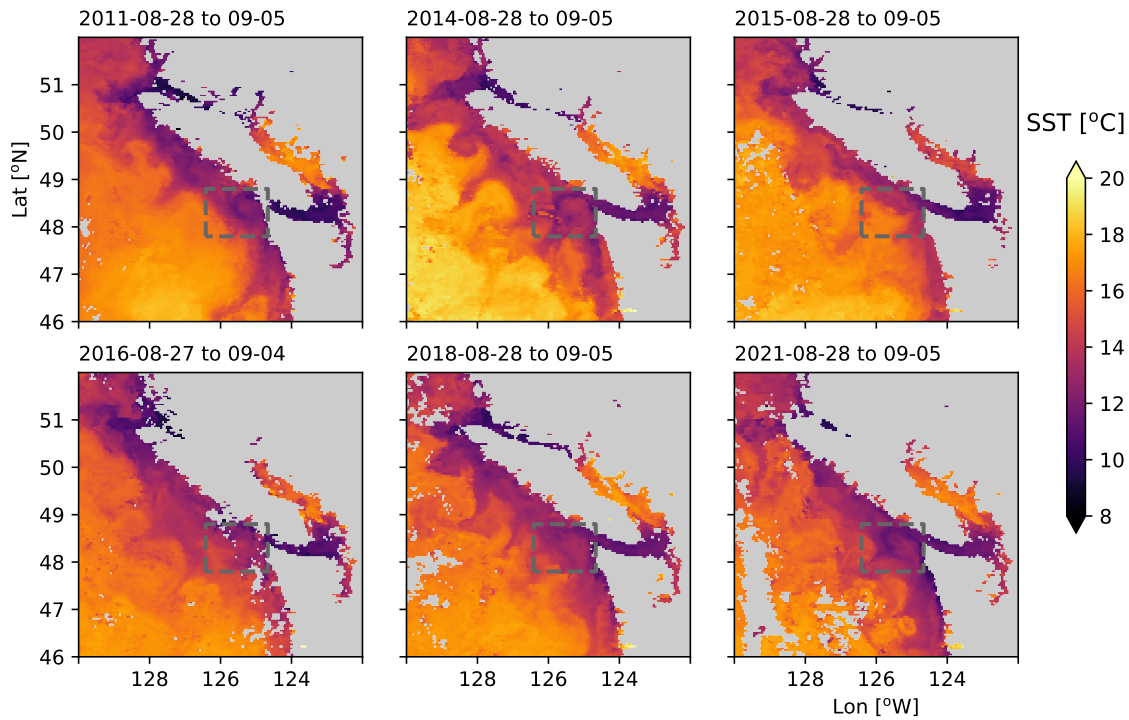


Figure 16. Late August sea-surface temperature, 8-day composites (NASA Ocean Biology Processing Group, 2019). From 2011 to 2021; missing years had too much cloud cover or no satellite coverage.

464 **Open Research**465 **Acknowledgments**

466 This section is optional. Include any Acknowledgments here.

467 **References**

- 468 Barth, J. A., Pierce, S. D., & Smith, R. L. (2000). A separating coastal upwelling jet at
 469 Cape Blanco, Oregon and its connection to the California Current system. *Deep Sea*
 470 *Res. II*, 47(5–6), 783 - 810. doi: [http://dx.doi.org/10.1016/S0967-0645\(99\)00127-7](http://dx.doi.org/10.1016/S0967-0645(99)00127-7)
- 471 Batteen, M. L. (1997). Wind-forced modeling studies of currents, meanders, and eddies in
 472 the California Current system. *J. Geophys. Res.*, 102(C1), 985–1010. doi: 10.1029/
 473 96jc02803
- 474 Brink, K. (2016). Cross-shelf exchange. *Annu. Rev. Mar. Sci.*, 8(1), 59–78. doi: 10.1146/
 475 [annurev-marine-010814-015717](https://doi.org/10.1146/annurev-marine-010814-015717)
- 476 Castelao, R. M., & Barth, J. A. (2007, nov). The role of wind stress curl in jet separation
 477 at a cape. *J. Phys. Oceanogr.*, 37(11), 2652–2671. doi: 10.1175/2007jpo3679.1
- 478 Dale, A. C., & Barth, J. A. (2001, jan). The hydraulics of an evolving upwelling jet flowing
 479 around a cape. *Journal of Physical Oceanography*, 31(1), 226–243. doi: 10.1175/
 480 1520-0485(2001)031(0226:thoaeu)2.0.co;2
- 481 Dewey, R. K., & Crawford, W. R. (1988). Bottom stress estimates from vertical dissipation
 482 rate profiles on the continental shelf. *J. Phys. Oceanogr.*, 18, 1167–1177.
- 483 DFO. (2022). *Marine environmental data section archive, buoy c46206*. Ecosystem and
 484 Oceans Science, Department of Fisheries and Oceans Canada. Retrieved 2022-01-31,
 485 from <https://meds-sdmm.dfo-mpo.gc.ca>
- 486 Dortch, Q., Rabalais, N. N., Turner, R. E., & Rowe, G. T. (1994, dec). Respiration rates
 487 and hypoxia on the Louisiana shelf. *Estuaries*, 17(4), 862. doi: 10.2307/1352754
- 488 Durski, S. M., & Allen, J. S. (2005). Finite-amplitude evolution of instabilities associated
 489 with the coastal upwelling front. *J. Phys. Oceanogr.*, 35(9), 1606–1628. doi: 10.1175/
 490 jpo2762.1
- 491 Engida, Z., Monahan, A., Ianson, D., & Thomson, R. E. (2016). Remote forcing of sub-
 492 surface currents and temperatures near the northern limit of the California Current
 493 system. *J. Geophys. Res.*, 121(10), 7244–7262. doi: 10.1002/2016jc011880
- 494 Foreman, M. G. G., Callendar, W., MacFadyen, A., Hickey, B. M., Thomson, R. E., &
 495 Lorenzo, E. D. (2008). Modeling the generation of the Juan de Fuca Eddy. *J.
 496 Geophys. Res.*, 113(C3). doi: 10.1029/2006jc004082
- 497 Freeland, H., & Denman, K. (1982). A topographically controlled upwelling ceter off
 498 southern Vancouver Island. *J. Mar. Res.*, 40(4), 1069–1093.
- 499 Freeland, H., & McIntosh, P. (1989). The vorticity balance on the southern British Columbia
 500 continental shelf. *Atmosphere–Ocean*, 27(4), 643–657.
- 501 Hickey, B., Thomson, R., Yih, H., & LeBlond, P. (1991). Velocity and temperature fluctua-
 502 tions in a buoyancy-driven current off Vancouver Island. *J. Geophys. Res.*, 96(C6),
 503 10,507–10,538.
- 504 Hu, C., Lee, Z., & Franz, B. (2012). Chlorophyll a algorithms for oligotrophic oceans: A
 505 novel approach based on three-band reflectance difference. *J. Geophys. Res.*, 117(C1).
 506 doi: 10.1029/2011jc007395
- 507 Ikeda, M., & Emery, W. J. (1984). A continental shelf upwelling event off Vancouver
 508 Island as revealed by satellite infrared imagery. *J. Mar. Res.*, 42(2), 303–317. doi:
 509 10.1357/002224084788502774
- 510 Ikeda, M., Mysak, L. A., & Emery, W. J. (1984). Observation and modeling of satellite-
 511 sensed meanders and eddies off Vancouver Island. *J. Phys. Oceanogr.*, 14(1), 3–21.
 512 doi: 10.1175/1520-0485(1984)014<0003:omso>2.0.co;2
- 513 Klymak, J. M., Shearman, R. K., Gula, J., Lee, C. M., D’Asaro, E. A., Thomas, L. N., ...
 514 others (2016). Submesoscale streamers exchange water on the north wall of the Gulf

- 515 Stream. *Geophys. Res. Lett.*. doi: 10.1002/2015GL067152
- 516 MacFadyen, A., & Hickey, B. M. (2010). Generation and evolution of a topographically
517 linked, mesoscale eddy under steady and variable wind-forcing. *Cont. Shelf Res.*,
518 30(13), 1387–1402. doi: 10.1016/j.csr.2010.04.001
- 519 Mackas, D. L., Denman, K. L., & Bennett, A. F. (1987). Least squares multiple tracer
520 analysis of water mass composition. *J. Geophys. Res.*, 92(C3), 2907–2918.
- 521 Mackas, D. L., & Yelland, D. R. (1999, nov). Horizontal flux of nutrients and plankton
522 across and along the British Columbia continental margin. *Deep Sea Res. II*, 46(11–
523 12), 2941–2967. doi: 10.1016/s0967-0645(99)00089-2
- 524 NASA Ocean Biology Processing Group. (2017). *MODIS-aqua level 3 mapped chloro-*
525 *phyll data version r2018.0*. NASA Ocean Biology DAAC. Retrieved from <https://oceancolor.gsfc.nasa.gov/data/10.5067/AQUA/MODIS/L3M/CHL/2018> doi: 10
526 .5067/AQUA/MODIS/L3M/CHL/2018
- 527 NASA Ocean Biology Processing Group. (2019). *MODIS-aqua level 3 mapped SST data*
528 *version r2019.0*. NASA Ocean Biology DAAC. Retrieved from https://oceandata.sci.gsfc.nasa.gov/ob/getfile/AQUA_MODIS
- 529 OSI SAF. (2015). *GHRSST level 2p sub-skin sea surface temperature from the Advanced*
530 *Very High Resolution Radiometer (AVHRR) on Metop satellites (currently Metop-A)*
531 *(GDS V2) produced by OSI SAF*. NASA Physical Oceanography DAAC. Retrieved
532 from https://podaac.jpl.nasa.gov/dataset/AVHRR_SST_METOP_A-OSISAF-L2P-v1.0 doi: 10.5067/GHAMA-2PO02
- 533 Pelland, N. A., Eriksen, C. C., & Lee, C. M. (2013). Subthermocline eddies over the
534 washington continental slope as observed by seagliders, 2003–09. *J. Phys. Oceanogr.*
535 doi: 10.1175/JPO-D-12-086.1
- 536 Relvas, P., & Barton, E. D. (2005). A separated jet and coastal counterflow during upwelling
537 relaxation off Cape São Vicente (Iberian Peninsula). *Cont. Shelf Res.*, 25(1), 29–49.
538 doi: 10.1016/j.csr.2004.09.006
- 539 Sahu, S., Allen, S. E., Saldías, G. S., Klymak, J. M., & Zhai, L. (2022, mar). Spatial and
540 temporal origins of the La Perouse low oxygen pool: A combined lagrangian statistical
541 approach. *J. Geophys. Res.*, 127(3). doi: 10.1029/2021jc018135
- 542 Thomson, R. E., & Gower, J. F. R. (1998, feb). A basin-scale oceanic instability event in
543 the gulf of alaska. *J. Geophys. Res.*, 103(C2), 3033–3040. doi: 10.1029/97jc03220
- 544 Thomson, R. E., Hickey, B. M., & LeBlond, P. H. (1989). The Vancouver Island Coastal
545 Current: Fisheries barrier and conduit. In R. J. Beamish & G. A. McFarlane (Eds.),
546 *Effects of ocean variability on recruitment and an evaluation of parameters used in*
547 *stock assessment models*. Fisheries and Oceans Canada.
- 548 Thomson, R. E., & Krassovski, M. V. (2015, dec). Remote alongshore winds drive variability
549 of the California Undercurrent off the British Columbia–Washington coast. *J. Geophys.*
550 *Res.*, 120(12), 8151–8176. doi: 10.1002/2015jc011306
- 551 Weaver, A. J., & Hsieh, W. W. (1987). The influence of buoyancy flux from estuaries
552 on continental shelf circulation. *J. Phys. Oceanogr.*, 17, 2127–2140. doi: 10.1175/
553 1520-0485(1987)017<2127:TIOBFF>2.0.CO;2